Supplemental Methods

Whole Exome Sequencing and Analysis

Genomic DNA was extracted using standard procedures. Targeted capture and massive parallel sequencing were performed at the UCSF Institute for Human Genetics. Briefly, genomic DNA was sheared by Covaris S2 (Woburn, MA) to a target size of 200-300bp and assembled into a library with TruSeq adapters containing indexes that differentiates different libraries in a capture reaction as well as a sequencing run (Kapa Biosystems, Wilmington, MA). Libraries were pooled into a capture reaction that contains biotinylated DNA oligonucleotides (called 'baits') from Roche-Nimblegen SeqCap EZ Human Exome Library v3.0 (Madison, WI) for 72 hours. The DNA bait-DNA hybrids were then pulled out of the complex mixture by incubation with streptavidin-labeled magnetic beads and captured onto a strong magnet. After washing, the targeted DNA of interest was eluted and subjected to 18 cycles of DNA amplification. Captured DNA libraries were sequenced with the Illumina HiSeq 2500 (Hayward, CA), yielding 150 (2X75) base pairs from the final library fragments. Sequence data were mapped to the GRCh37 reference genome and analyzed using the Ingenuity Variant Analysis platform (Qiagen, Venlo, Netherlands). Variants identified by whole exome sequencing were filtered using three criteria (see also Supplemental Figure 2). First, only variants with an allele frequency consistent with published reports of hereditary CP prevalence (<0.001%) within the Genome Aggregation Database (gnomAD) database were kept. gnomAD is a highly annotated, searchable database of 141,456 human exome and genome sequences (1). Second, only variants with a scaled Combined Annotation-Dependent Depletion (CADD) score >20 were selected. The scaled CADD score is an

integrative annotation built from more than 60 genomic features, and variants with a scaled CADD score of >20 are predicted to be in the top 1% of deleterious variants in the human genome (2). Third, only variants that cosegregated with disease were kept. Sanger sequencing was performed using standard methods. Primers used for Sanger sequencing of *CELA3B*, *FOXN1*, *PRSS1* and *TJP2* variants can be found in Supplemental Table 1.

Mutagenesis of Human Elastases

p.R90C (c.C268>T) CELA3B, p.R90L (c.G269>T) CELA3B, p.S217A (c.T649>G) CELA3B, p.L90R (c.T269>G) CELA3A and p.L90C (c.C268>T, T269>G) CELA3A mutagenesis were achieved using the Quikchange Lightning Site-directed mutagenesis kit (Agilent Technologies) and previously published (3, 4) untagged and 9xHis-tagged *CELA3B* and *CELA3A* constructs in pcDNA3.1(-) plasmids (gifts from Miklos Sahin-Toth, Boston University, Boston, MA). CELA3B variants without signal peptides (ΔSP) were generated by sequentially removing two potential start codons (No start) and converting p.A15 to p.M15 (New start) to introduce a start codon at the beginning of the pro-domain. All mutagenesis primer sequences are available in Supplemental Table 3 (Integrated DNA Technologies). Sanger sequencing of the all plasmids was performed by Quintara Biosciences using T7 Forward and BGH Reverse primers.

Tissue Culture and Western Blotting

HEK 293T cells (5)(gift from Feroz Papa at UCSF) were cultured in DMEM media supplemented with 10% FBS (Gemini Bioproducts), 100 U/mL penicillin, and 100 ug/mL streptomycin (UCSF Cell Culture Facility). All expression constructs were transfected into ~25% confluent HEK 293T cells using Opti-MEM and Lipofectamine 2000 (ThermoFisher Scientific). For protein analysis, cells were lysed in M-PER buffer (Thermo Fisher Scientific) plus phosphatase inhibitor cocktail (Cell Signaling Technologies) and protein concentration was determined using Pierce BCA Protein Assay (Thermo Fisher Scientific). For secreted protein, conditioned media was directly collected and cleared by centrifugation. Western blots were performed using 10% Bis-Tris precast SDS-PAGE gels (NuPage) on Invitrogen XCell SureLock Mini-Cell modules. Gels were run using 2-(N-morpholino)ethanesulfonic acid (MES) buffer (Invitrogen) and transferred onto nitrocellulose transfer membrane using an XCell II Blot Module or iBlot Dry Blotting System (Thermo Fisher Scientific). Antibody binding was visualized and quantified using the Odyssey CLx Imaging System (LI-COR Biosciences). Antibodies used: CELA3B (Sigma SAB1409028; 1:1,000), 6x-His Tag (ThermoFisher Scientific MA1-21315; 1:1,000), CPA1 (R&D Systems MAB 2856; 1:500), CPA2 (R&D Systems AF2896; 1:500), and β-actin (Sigma A5441; 1:3,000).

RNA Isolation and Quantitative Real-Time PCR

RNA was isolated from whole cells using Qiashredder and RNeasy kits (Qiagen). For cDNA synthesis, 500-1000 ng total RNA was reverse transcribed using Superscript II Reverse Transcriptase and Oligo $d(T)_{16}$ primer (Invitrogen). For qPCR, we used Power

SYBR Green and the StepOnePlus Real-Time PCR System (Applied Biosystems). qPCR primers are listed in Supplemental Table 4 (Integrated DNA Technologies). Gene expression levels were normalized to β-actin.

Protein Purification and Catalytic Assays

Production, purification and catalytic analysis of CELA3B have been previously described (3). Briefly, HEK 293T cells transiently expressing 9xHis-tagged CELA3B variants were placed in Opti-MEM for two days and the resulting conditioned media incubated with Complete His-Tag Purification Resin (Roche) to isolate His-tagged proteins. Purified CELA3B-9xHis variants were eluted from the resin in the presence of 500 mM imidazole, dialyzed into Elastase Buffer (100 mM Tris 8.0, 1 mM $CaCl_2$) using Slide-A-Lyzer Dialysis Cassettes (ThermoFisher Scientific), and concentrated using Amicon Ultra-4 Centrifugal Filter Units (Millipore). CELA3B concentrations were determined by running on 10% Bis-Tris SDS-PAGE gels, staining with Coomassie Brilliant Blue (ThermoFisher Scientific) and comparing to a bovine serum albumin (BSA) standard curve; protein concentrations were insufficient for analysis by BCA. Purified elastases were diluted to equal concentrations and proteolytically activated using Immobilized TPCK-Trypsin resin (ThermoFisher Scientific) for four hours at 4°C. Active elastases were incubated against a logarithmic concentration gradient of Succinyl-Ala-Ala-Pro-Ala-pNA (S-A-A-P-A-pNa; Bachem) and absorbance at 405 nm (A405) was measured over time. For each CELA3B variant, raw absorbance values were compared to a 4-nitroaniline (Sigma) standard curve to calculate their rates of proteolysis at each substrate concentration and, in accordance with Michaelis-Menten

enzyme kinetics, their catalytic rate (k_{cat}) and Michaelis (Km) constants. To measure activation efficiency of CELA3B variants, conditioned media were concentrated 20x and directly applied to Immobilized TPCK-Trypsin resin for three hours at 4°C. The partially activated proteins were incubated with 800 nM S-A-A-P-A-pNa to obtain A405 values and relative rates of catalysis were normalized to CELA3B protein levels as determined by coomassie staining.

CELA3B and CPA1/2 Binding Assay

His-tagged CELA3B variants and untagged CPA1 and CPA2 (gifts from Miklos Sahin-Toth, Boston University, Boston, MA) were transiently expressed in HEK 293T cells and conditioned media was collected. Secreted levels of CELA3B variants were determined by Western blot and concentrations were leveled using conditioned media from mock-transfected cells. CELA3B variants were individually combined with CPA1 or CPA2 at a 1:1 ratio, bound to His-tag purification resin, and eluted with imidazole as described above. Indicated fractions were analyzed by Western blot for CELA3B, CPA1 and CPA2.

Pulse-Chase Analysis of CELA3B Expression

HEK 293T cells transiently expressing 9xHis-tagged CELA3B variants were starved for 30 minutes in serum-, methionine- and cysteine-free DMEM (ThermoFisher Scientific) before incubation with serum-free media containing ^{35}S-labeled methionine and cysteine (Perkin Elmer). For secretion studies, cells were pulsed with radiolabeled amino acids for one hour at room temperature before chasing with “cold” serum-free media and

collecting at the indicated time points. For degradation/stability studies, cells were pulsed and chased in the presence of 0.5 μg/mL Brefeldin A (BFA; Cell Signaling Technology 9972) to prevent protein secretion and collected at the indicated time points. For synthesis/translation studies, cells were pulsed (no chase) in the presence of BFA and collected at the indicated time points. Cells were lysed using M-PER and CELA3B-9xHis isolated using Complete His-Tag Purification Resin (Roche). Isolated proteins were denatured and run on 10% Bis-Tris SDS-PAGE gels, dried under vacuum, and analyzed by autoradiography and densitometry (ImageJ; U.S. National Institutes of Health).

Generation of Cela3b Mutant Mice By CRISPR-Cas9

To generate *Cela3b* mutant mice, we obtained purified Cas9, a *Cela3b*-targeting guide RNA (gRNA; 5'-CACCTACCAGGTTGTACTTG-3') that targets Cas9 to a site near the R89 codon, and donor oligos for homology directed repair (HDR) resulting in p.R89C (c.C265>T) or p.R89L (c.G266T) mutations (HDR donor sequences available in Supplemental Table 5). Purified Cas9 and *Cela3b*-targeting gRNA were procured from PNA Bio; HDR oligos were obtained from Integrated DNA Technologies. All three products were injected into C57BL/6 zygotes at the Transgenic Gene Targeting Core in the Gladstone Institutes. The resulting pups were genotyped by amplifying a 496 bp region flanking the R89 site with the KAPA Mouse Genotyping Kit (KAPA Biosystems) and subsequent Sanger sequencing at Quintara Biosciences using the reverse primer (see Supplemental Table 1 for primer sequences). To expunge unlinked, off-target Cas9 modifications, three mutant founders were selected for each *Cela3b* variant and

backcrossed to genetically pure C57BL/6NJ mice (Jackson Laboratory) for three generations. Heterozygous mice from each founder line were then intercrossed to produce litters with WT, heterozygous, and homozygous animals.

Induction of Pancreatitis and Pancreatic Histological Quantification

To chemically induce pancreatitis, 20-week-old mice were given eight hourly injections of vehicle (PBS) or 75 μg/kg caerulein (Bachem) per day for two consecutive days. 7 days after the final injection, mice were euthanized and their pancreata were fixed in formalin, embedded in paraffin, and H&E stained. Pancreatic damage was quantified by scoring at least 9 randomly chosen high-powered fields per mouse in a blinded fashion. Tissue integrity, acinar de-differentiation and immune infiltration were scored from (0-5) and individual scores for these three categories were added to make a combined score as previously described (6).

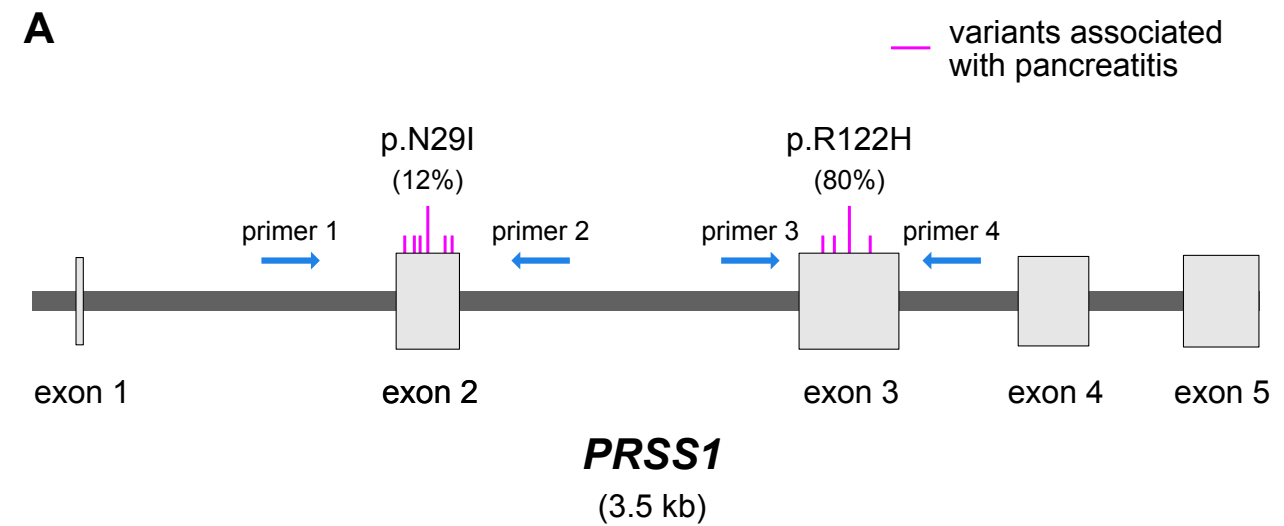
A
variants associated with pancreatitis
p.N29I
(12%)
p.R122H
(80%)
primer 1
primer 2
primer 3
primer 4
exon 1
exon 2
exon 3
exon 4
exon 5
PRSS1
(3.5 kb)

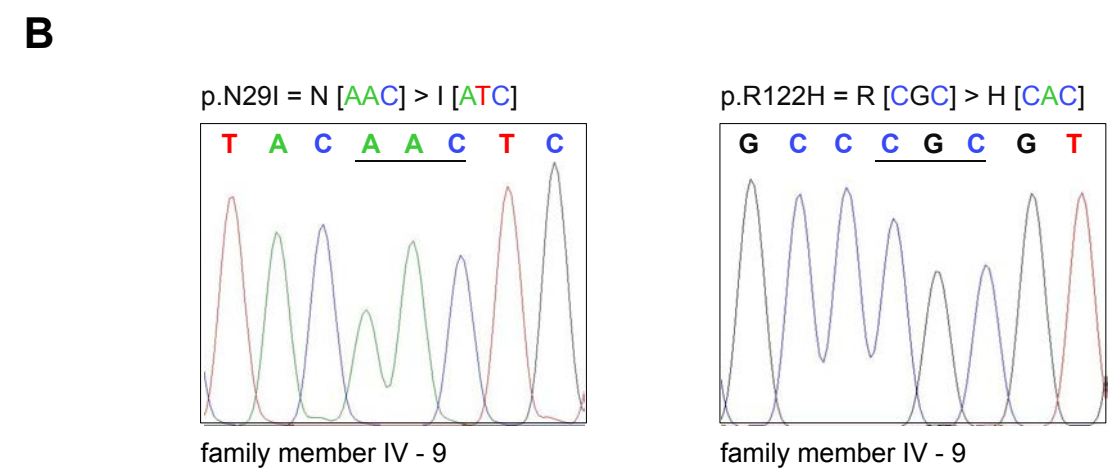
B
p.N29I = N [AAC] > I [ATC]
T A C A A C T C
family member IV - 9
p.R122H = R [CGC] > H [CAC]
G C C C G C G T
family member IV - 9

Figure S1

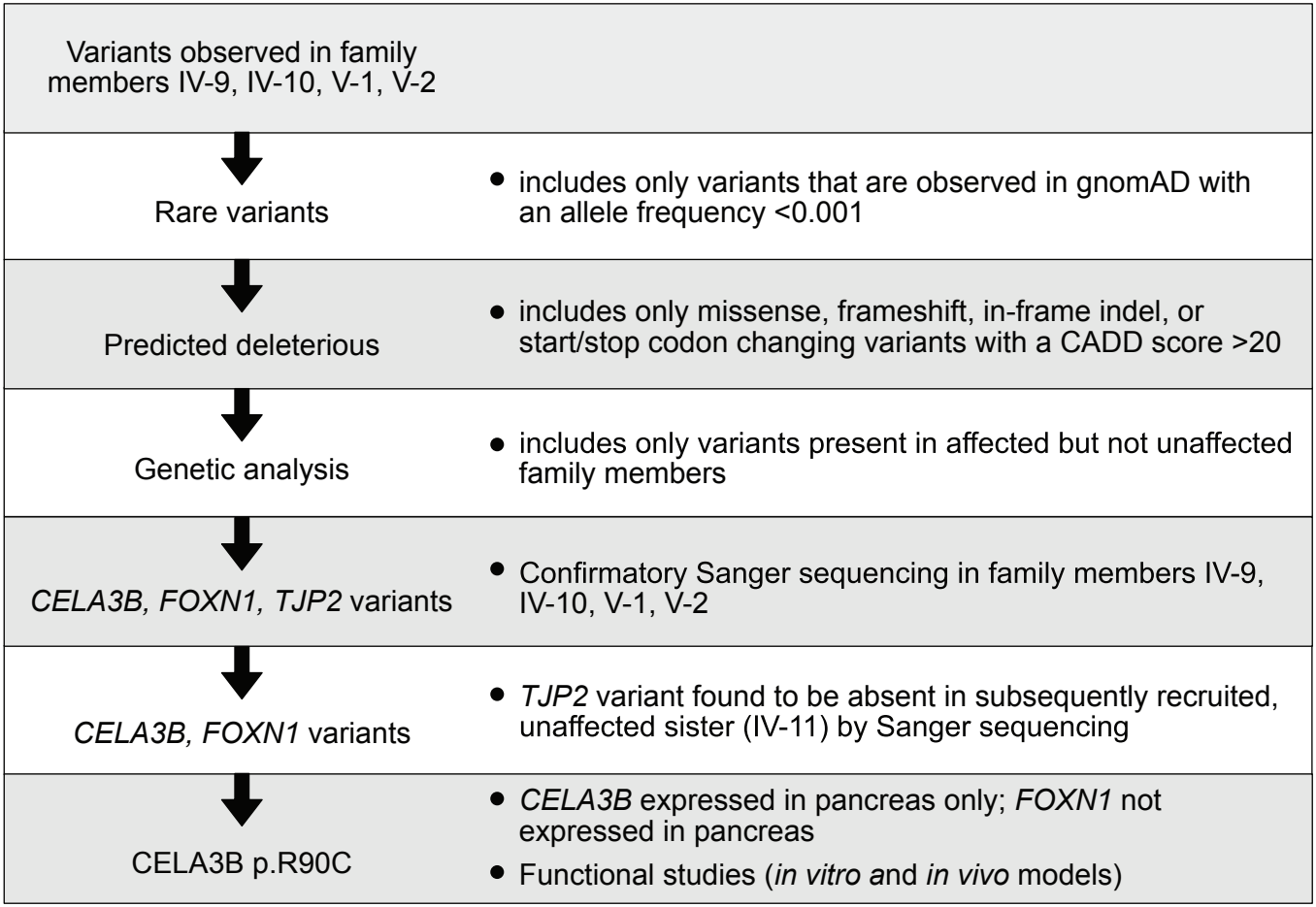
Variants observed in family members IV-9, IV-10, V-1, V-2
Rare variants
includes only variants that are observed in gnomAD with an allele frequency <0.001
Predicted deleterious
includes only missense, frameshift, in-frame indel, or start/stop codon changing variants with a CADD score >20
Genetic analysis
includes only variants present in affected but not unaffected family members
CELA3B, FOXN1, TJP2 variants
Confirmatory Sanger sequencing in family members IV-9, IV-10, V-1, V-2
CELA3B, FOXN1 variants
TJP2 variant found to be absent in subsequently recruited, unaffected sister (IV-11) by Sanger sequencing
CELA3B p.R90C
CELA3B expressed in pancreas only; FOXN1 not expressed in pancreas
Functional studies (in vitro and in vivo models)

Figure S2

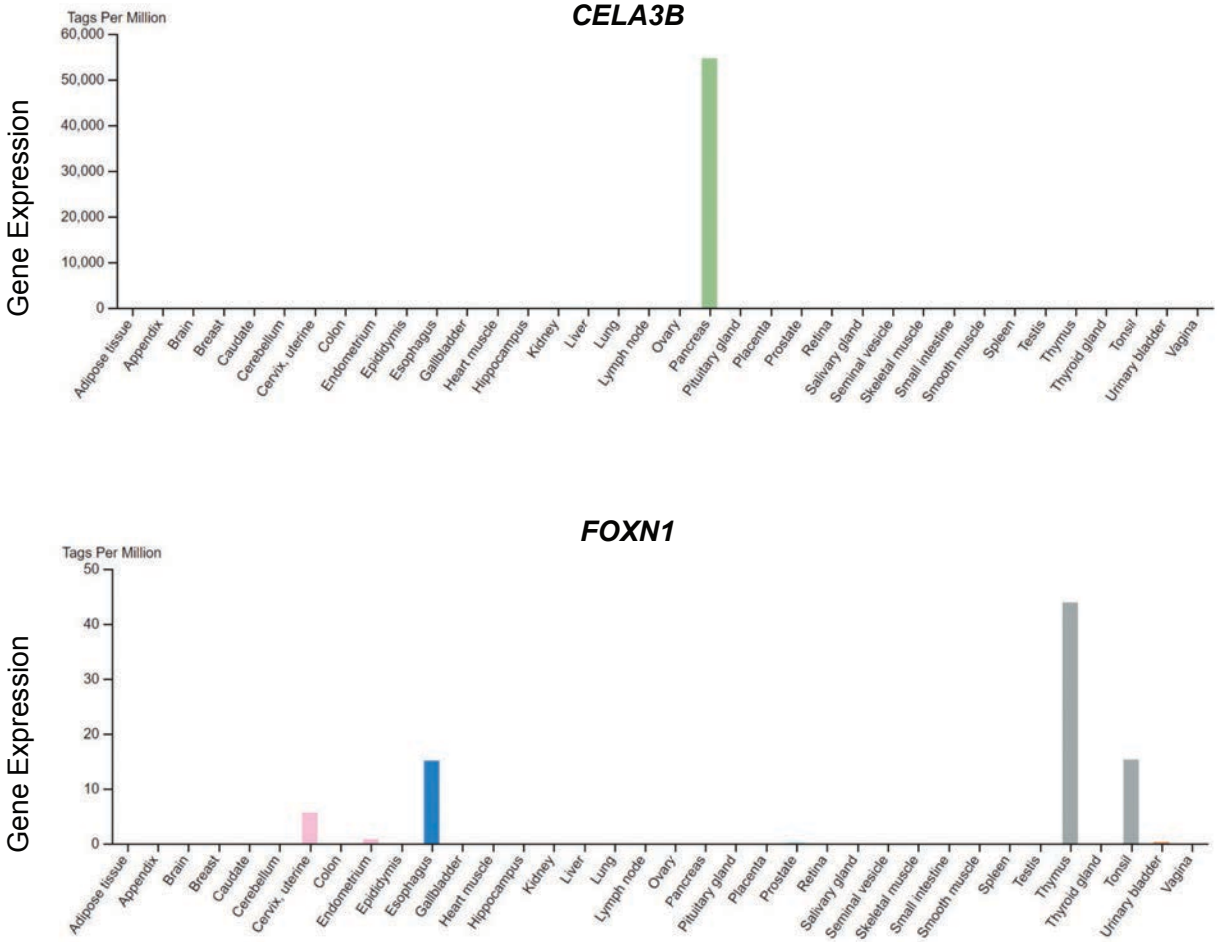
CELA3B
Tags Per Million
Gene Expression
60,000
50,000
40,000
30,000
20,000
10,000
0
Adipose tissue
Appendix
Brain
Breast
Caudate
Cerebellum
Cervix, uterine
Colon
Endometrium
Epididymis
Esophagus
Gallbladder
Heart muscle
Hippocampus
Kidney
Liver
Lung
Lymph node
Ovary
Pancreas
Pituitary gland
Placenta
Prostate
Retina
Salivary gland
Seminal vesicle
Skeletal muscle
Small intestine
Smooth muscle
Spleen
Testis
Thymus
Thyroid gland
Tonsil
Urinary bladder
Vagina
FOXN1
Tags Per Million
Gene Expression
50
40
30
20
10
0
Adipose tissue
Appendix
Brain
Breast
Caudate
Cerebellum
Cervix, uterine
Colon
Endometrium
Epididymis
Esophagus
Gallbladder
Heart muscle
Hippocampus
Kidney
Liver
Lung
Lymph node
Ovary
Pancreas
Pituitary gland
Placenta
Prostate
Retina
Salivary gland
Seminal vesicle
Skeletal muscle
Small intestine
Smooth muscle
Spleen
Testis
Thymus
Thyroid gland
Tonsil
Urinary bladder
Vagina

Figure S3

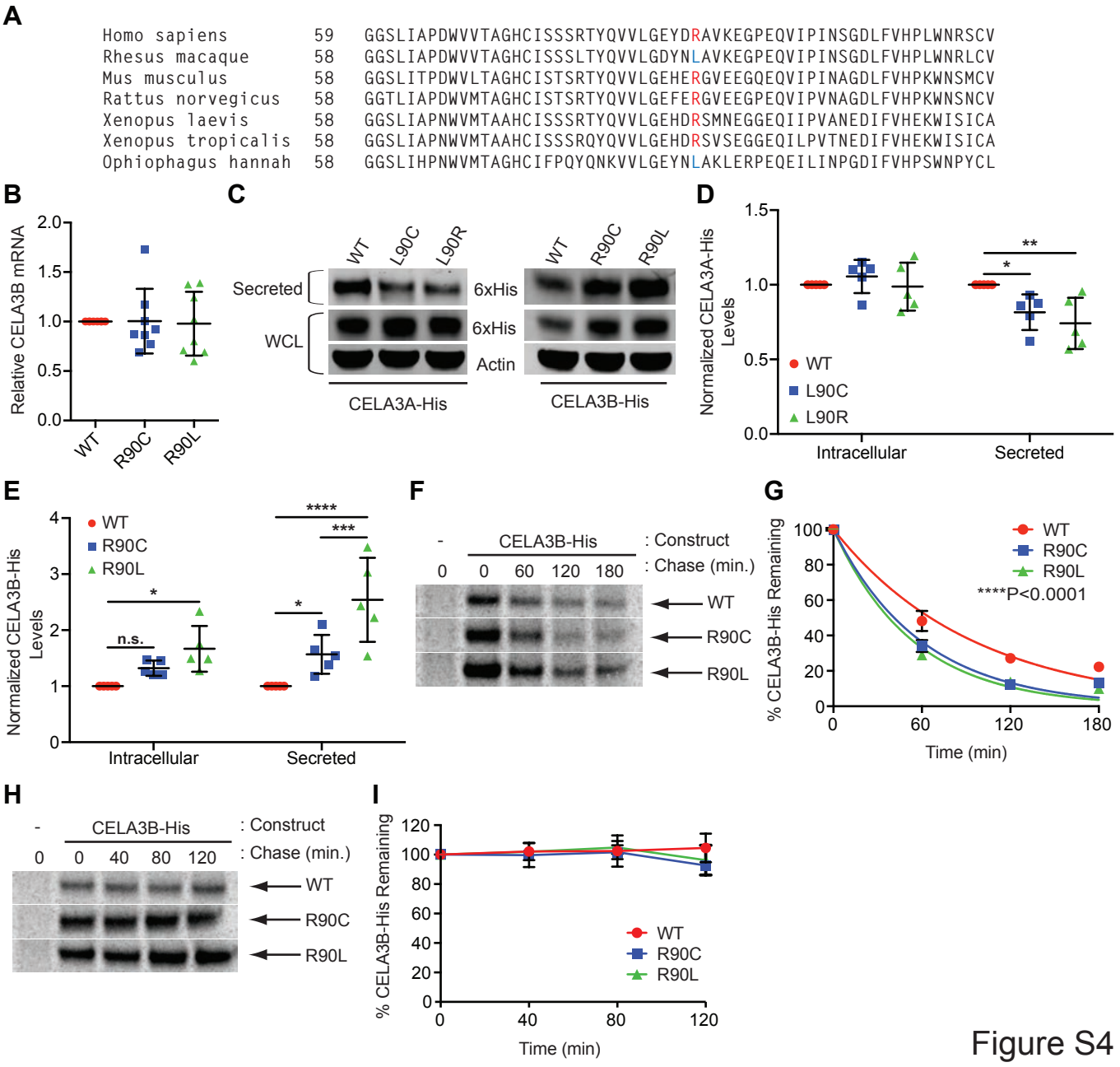
A
Homo sapiens 59 GGSLIAPDWVVTAGHCISSSRTYQVVLGEYDRAVKEGPEQVIPINSGDLFVHPLWNRSCV
Rhesus macaque 58 GGSLIAPDWVVTAGHCISSSLTYQVVLGDYNLAVKEGPEQVIPINSGDLFVHPLWNRLCV
Mus musculus 58 GGSLITPDWVLTAGHCISTSRTYQVVLGEHERGVEEGQEQVIPINAGDLFVHPKWNSMCV
Rattus norvegicus 58 GGTLIAPDWVMTAGHCISTSRTYQVVLGEFERGVEEGPEQVIPVNAGDLFVHPKWNSNCV
Xenopus laevis 58 GGSLIAPNWVMTAAHCISSSRTYQVVLGEHDRSMNEGGEQIIPVANEDIFVHEKWISICA
Xenopus tropicalis 58 GGSLIAPNWVMTAAHCISSSRQYQVVLGEHDRSVSEGGEQILPVTNEDIFVHEKWISICA
Ophiophagus hannah 58 GGSLIHPNWVMTAGHCIFPQYQNKVVLGEYNLAKLERPEQEILINPGDIFVHPSWNPYCL
B
Relative CELA3B mRNA
2.0
1.5
1.0
0.5
0.0
WT
R90C
R90L
C
WT
L90C
L90R
Secreted
WCL
6xHis
6xHis
Actin
CELA3A-His
WT
R90C
R90L
CELA3B-His
D
Normalized CELA3A-His Levels
1.5
1.0
0.5
0.0
**
*
WT
L90C
L90R
Intracellular
Secreted
E
Normalized CELA3B-His Levels
4
3
2
1
0
WT
R90C
R90L
****
***
*
*
n.s.
Intracellular
Secreted
F
-
CELA3B-His
: Construct
0
0
60
120
180
: Chase (min.)
WT
R90C
R90L
G
% CELA3B-His Remaining
100
80
60
40
20
0
WT
R90C
R90L
****P<0.0001
0
60
120
180
Time (min)
H
-
CELA3B-His
: Construct
0
0
40
80
120
: Chase (min.)
WT
R90C
R90L
I
% CELA3B-His Remaining
120
100
80
60
40
20
0
WT
R90C
R90L
0
40
80
120
Time (min)

Figure S4

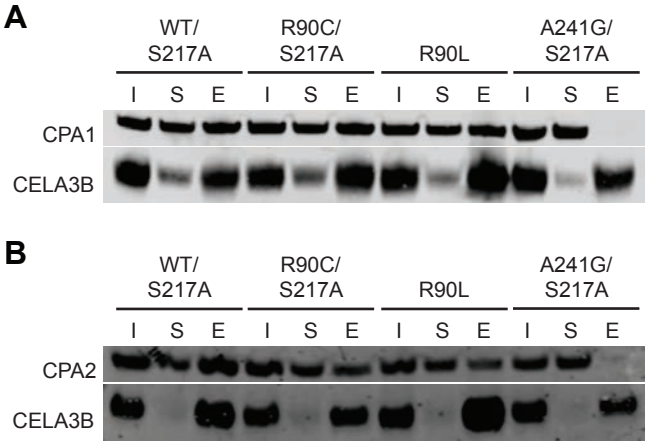
A
WT/
S217A
R90C/
S217A
R90L
A241G/
S217A
I S E I S E I S E I S E
CPA1
CELA3B
B
WT/
S217A
R90C/
S217A
R90L
A241G/
S217A
I S E I S E I S E I S E
CPA2
CELA3B

Figure S5

Supplemental Figure Legends

Supplemental Figure 1: Sanger sequencing of exons 1 and 2 of *PRSS1*. (**A-C**) (**A**) Diagram of the *PRSS1* locus and variants commonly associated with hereditary pancreatitis. Up to 80% of people with hereditary CP have a mutation in the *PRSS1* gene, which encodes the most abundant trypsinogen secreted by the pancreas; *PRSS1* variants p.R112H and p.N29I account for >90% of *PRSS1* mutations associated with hereditary CP. (**B**) Chromatograms flanking the codons for N29 and R122 in the proband. Sanger sequencing of *PRSS1* exons 2 and 3 confirmed the absence of p.R112H, p.N29I and other previously associated pancreatitis variants in family members.

Supplemental Figure 2: Flow chart of whole exome sequencing and variant analysis. Variants were initially filtered based on rarity, likelihood to be deleterious (CADD score), and cosegregation with disease. Sanger sequencing, tissue expression profiling and extensive functional studies confirmed that c.C268>T (p.R90C) in *CELA3B* is the disease causing variant in this family. Detailed methods are provided in the Supplementary Appendix.

Supplemental Figure 3: Expression of *CELA3B* and *FOXN1* in humans. RNA expression overview across different human tissues shows selective expression of *CELA3B* in the pancreas; *FOXN1* is not expressed in the pancreas (7).

Supplemental Figure 4: Additional functional characterization of CELA3B mutations at arginine 90. (**A-I**) (**A**) Sequence alignment of verified CELA3B sequences from seven different species; alignments are centered on R90 from human CELA3B and labeled as in Figure 2A. (**B**) Quantitative reverse transcription polymerase chain reaction (RT-qPCR) quantification of *CELA3B* transcripts from samples in Figure 2B and C. (**C**) Immunoblots of His-tagged CELA3A and CELA3B variants. Samples are whole cell lysates (intracellular) and conditioned media (secreted protein) from 293T cells transfected with empty vector (Mock) or vector containing the indicated gene. Blots were probed with the indicated antibodies. (**D**) Quantification of CELA3A variant data from n=5 experiments as in C; normalized to WT CELA3A. Values are means ± SD. (**E**) Quantification of CELA3B data from n=5 experiments as in C; normalized to WT CELA3B. Values are means ± SD**.** (**F**) Autoradiographs of His-tagged CELA3B variants purified from untreated 293T cells pulsed with ^{35}S-labeled methionine and cysteine and chased with unlabeled amino acids for the indicated amounts of time. First (control) lane is the same in WT and R90C images. (**G**) Quantification of n=4 experiments as in F, showing the percentage of each CELA3B variant remaining over the time course. Values for each time point are means ± SD; exponential (one phase) decay used to model curves. P<0.0001 when comparing WT and either mutant. (**H**) Autoradiographs of His-tagged CELA3B variants purified from Brefeldin A-treated 293T cells pulsed with ^{35}S-labeled methionine and cysteine and chased with unlabeled amino acids for the indicated amount of time. First (control) lane is the same in WT and R90C images. (**I**) Quantification of n= 4 unique experiments as in H, showing the percentage of each CELA3B variant remaining over the time course. Values for each time point are means

± SD. P values were determined by matched 1-way ANOVA (panel C) or matched 2-way ANOVA (panels D and E) with Tukey's multiple comparisons test; *P<0.05, **P<0.01, ***P<0.001 and ****P<0.0001.

Supplemental Figure 5: Binding of CELA3B variants to CPA1 and CPA2. (A) Immunoblots of affinity-purification fractions using the indicated variants of His-tagged CELA3B in the presence of CPA1. (B) Immunoblots as in A, but in the presence of CPA2. Fractions are input (I), supernatant (S) and eluate (E). Where shown, catalytically dead (S217A) CELA3B variants were used to improve yield without affecting binding efficiency (4). All blots are representative of n=3 experiments.

Supplemental Tables

Table S1. Sanger Sequencing Primers

Target Gene	Forward Primer	Reverse Primer
CELA3B	TGGGGAGGCTTTGGAGAATCAG	CTGTGGGTCATGGAGGGATGAG
***Cela3b* (Mouse)**	CCACCAGGTCTCCCTTCAGTA	GGGCTAGAGCCTTAAGCTACCAT
FOXN1	ATGGGAGAGTGTTGTGGGTCAG	TTTGGCTCATGAGTACCCTGGG
***PRSS1* Exon 2**	CCTAGCTTGGCAAAAGAATC	TGCCTGCTTTTCTCACTAGCT
***PRSS1* Exon 3**	CACCCCACTACCACCAAC	CTCGAAATGTGTCTTAAGCCT
TJP2	AGAGGTGGCAAGAGCAGCATAA	TGACGGGATGTTGATGAGGGTC

Table S2. CELA3B Enzyme Kinetics*

CELA3B	K_m (μM)	P	k_{cat} (s^{-1})	P	k_{cat}/K_m ($M^{-1}s^{-1}$)	P
WT	311.7 ±0.6	-	14.6 ±0.5	-	$4.7x10^4$ $\pm1.4x10^3$	-
R90C	306.4 ±32.3	NS	14.6 ±0.5	NS	$4.8x10^4$ $\pm3.8x10^3$	NS
R90L	245.2 ±23.5	NS	14.9 ±1.7	NS	$6.1x10^4$ $\pm1.2x10^3$	<0.05

*Values are averages of n=3 experiments ± SD. Statistical significance for each constant was assessed by matched 1-way ANOVA with Tukey's multiple comparisons test; multiplicity-adjusted P values reported.

Table S3. Mutagenesis Primers

Mutation	Forward Primer	Reverse Primer
CELA3B p.R90C	TGGGCGAGTACGACTGTGCTGTGAAGGAG	CTCCTTCACAGCACAGTCGTACTCGCCCA
CELA3B p.R90L	TGGGCGAGTACGACCTTGCTGTGAAGGAG	CTCCTTCACAGCAAGGTCGTACTCGCCCA
CELA3A p.L90R	GGGTGAGTACAACCGTGCTGTGAAGGAGG	CCTCCTTCACAGCACGGTTGTACTCACCC
CELA3A p.L90C	GGGTGAGTACAACTGTGCTGTGAAGGAGG	CCTCCTTCACAGCACAGTTGTACTCACCC
CELA3B ΔSP No Start	CATCGCAAAACTCATAGTGCTCCGGCTGCTC	GAGCAGCCGGAGCACTATGAGTTTTGCGATG
CELA3B ΔSP New Start	CTCCTTGTGGCCGTTATGTCAGGCTATGGCCCAC	GTGGGCCATAGCCTGACATAACGGCCACAAGGAG
CELA3B p.S217A	CTGCAATGGTGACGCTGGAGGACCCCT	AGGGGTCCTCCAGCGTCACCATTGCAG

Table S4. qPCR Primers

Target mRNA	Forward Primer	Reverse Primer
β-Actin	GCAAATGCTTCTAGGCGGAC	AAGAAAGGGTGTAAAACGCAGC
CELA3B	TGAGGATGCGGTCCCCTA	GTGGCCCGTTGGTATAGAGA

Table S5. CRISPR HDR Donor Oligos

Cela3b Mutation	Donor Oligo Sequence
p.R89C	AGAGTTCCACTTGGGGTGCACAAAGAGGTCTCCAGCGTTGATGGGGATCACCTGTTCTTGGCCTTCCTCCACACCACATTCATGCTCGCCAAGTACAACCTGGTAGGTGCGAGAAGTCCTGCGGAAGAGTGGAGGTCAGTATAAGCCTGGAGC
p.R89L	AGAGTTCCACTTGGGGTGCACAAAGAGGTCTCCAGCGTTGATGGGGATCACCTGTTCTTGGCCTTCCTCCACACCAAGTTCATGCTCGCCAAGTACAACCTGGTAGGTGCGAGAAGTCCTGCGGAAGAGTGGAGGTCAGTATAAGCCTGGAGC

Supplemental References

1. Lek M, Karczewski KJ, Minikel EV, Samocha KE, Banks E, Fennell T, O'Donnell-Luria AH, Ware JS, Hill AJ, Cummings BB, et al. Analysis of protein-coding genetic variation in 60,706 humans. *Nature.* 2016;536(7616):285-91.
2. Ng PC, and Henikoff S. SIFT: Predicting amino acid changes that affect protein function. *Nucleic acids research.* 2003;31(13):3812-4.
3. Szabo A, and Sahin-Toth M. Determinants of chymotrypsin C cleavage specificity in the calcium-binding loop of human cationic trypsinogen. *The FEBS journal.* 2012;279(23):4283-92.
4. Szabo A, Pilsak C, Bence M, Witt H, and Sahin-Toth M. Complex Formation of Human Proelastases with Procarboxypeptidases A1 and A2. *The Journal of biological chemistry.* 2016;291(34):17706-16.
5. DuBridge RB, Tang P, Hsia HC, Leong PM, Miller JH, and Calos MP. Analysis of mutation in human cells by using an Epstein-Barr virus shuttle system. *Mol Cell Biol.* 1987;7(1):379-87.
6. Folias AE, Penaranda C, Su AL, Bluestone JA, and Hebrok M. Aberrant innate immune activation following tissue injury impairs pancreatic regeneration. *PloS one.* 2014;9(7):e102125.
7. Uhlen M, Fagerberg L, Hallstrom BM, Lindskog C, Oksvold P, Mardinoglu A, Sivertsson A, Kampf C, Sjostedt E, Asplund A, et al. Proteomics. Tissue-based map of the human proteome. *Science.* 2015;347(6220):1260419.